A minimal hardware implementation of a high speed ERT system and a demonstration of its capabilities

E.W. Randall[1], K.H. Hauslaib[2], O. Adetunji[1]

[1]Chemical Engineering, University of Cape Town
[2]Electrical Engineering, University of Cape Town
E-mail: bill.randall@uct.ac.za

ABSTRACT

Since the validity of the UCT current pulse technique for ERT measurements was established, the intention was to provide a low cost and simple to construct instrument using commonly available electronic components. The most recent versions of electronic circuits to provide this function have recently been published. The practical implementation has now been reduced to two easy to assemble circuit boards, i.e. a 16 channel amplifier and a second board incorporating the current source and electrode selection multiplexers. In addition, the system requires a microcontroller to implement the programmed electrode selection sequence and current pulse timing. A commercially available DAQ is used to record the voltage measurements and transmit them to an embedded PC for real-time image reconstruction and storage for further offline processing. This system can record adjacent pairs data frames from a single 16 electrode ring at 850 frames/second, or at a proportionally reduced rate from up to 4 electrode rings simultaneously. This paper describes the hardware and discusses the performance of the system. Some data is presented which demonstrates the use of the system in the determination of gas distribution in a bubble column and complements actual bubble size distribution determined with an optical detection probe.

Keywords ERT, Hardware, Bubbles, Flotation

1 INTRODUCTION

The UCT ERT system implements a current pulse technique which was first proposed by Randall et al (2001). The benefit of this method is that it relies on the measurement of the amplitude of a square-wave on the measurement electrode pairs resulting from the injection of a bi-directional constant current pulse on the excitation electrode pair. The electronics to implement this function is simpler than required for AC excited systems and has been shown to yield similar results by Stephenson (2007). Capture rates of up 1000 frames/second have been achieved for the adjacent pairs strategy using a single ring of 16 electrodes.

During the development of the system, many configurations of the instrument have been constructed. A system which allows up to 8 rings of 16 electrodes, with multiplexing to allow "cross-layer" current injection and measurement, has been described by Wilkinson et al (2006). More recently, development has been directed towards a low cost and easily constructed reliable system which is primarily targeted at slurry pipe-line flow measurements related to fluidisation of the slurry and velocity profile measurements (using cross correlation) where ERT data frames from independent electrode layers are adequate. Many other applications, in which the medium under investigation is primarily resistive, are possible. The electronics to implement this were described by Randall et al (2010). The restrictions in this design are related to the multiplexing system, but result in significant simplification of the circuitry and construction. The circuit boards used in the instrument described in that paper have been further simplified, with some improvement in performance. The ERT functions are now implemented on only two double sided printed circuit boards: 1) the current source and multiplexers, and 2) a 16 channel differential amplifier with sample and holds. In addition, the system requires an MCU to control the multiplexers and a commercially available DAQ for recording the voltages from the amplifier. The data sets are streamed to an embedded

"Wafer" PC (Intel Atom CPU) for real-time reconstruction (currently 2D, adjacent pairs only) and recording for off-line processing.

2 ELECTRONICS HARDWARE

The configuration of the system is shown in Figure 1. The ERT functions are implemented on only two circuit boards (PCB 1 and PCB 2 shown in Figure 2). The additional digital circuitry (MCU, DAQ and PC) is required to control the system and record and process the data sets acquired. A complete assembled system (without the Wafer PC) is shown in Figure 3 and a typical output screen from the PC is shown in Figure 4.

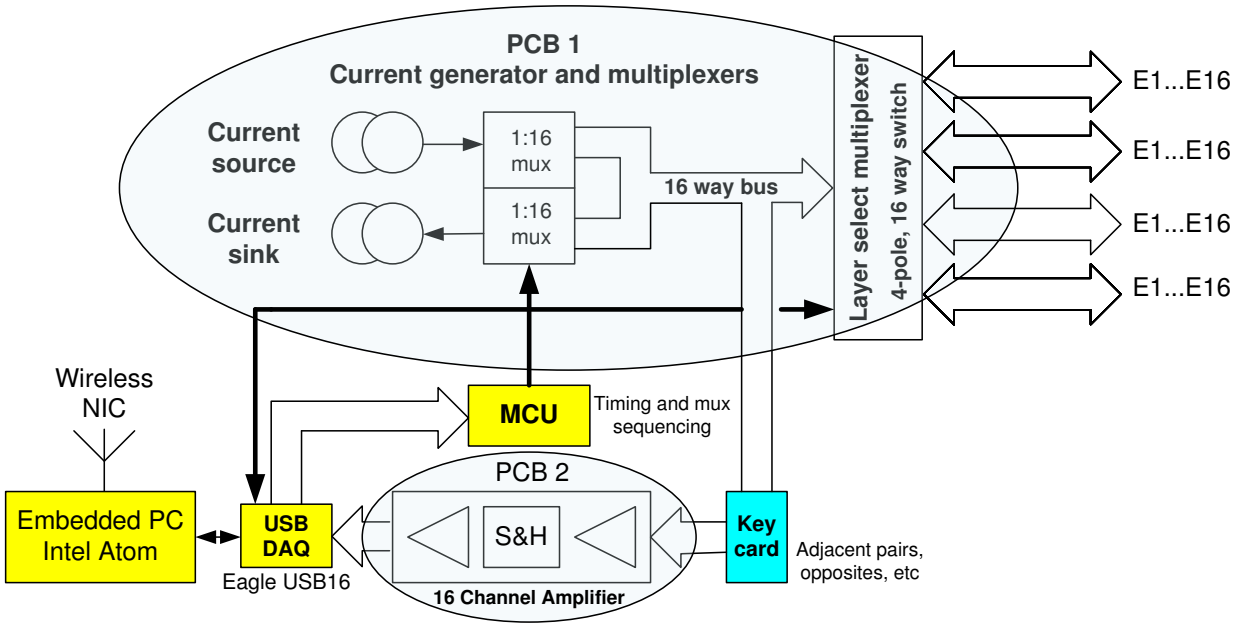

Figure 1: Configuration of ERT system implemented on two circuit boards, PCB1: the current source / mux and PCB2: the 16 channel amplifier. In addition, an MCU is required to control the electrode selection multiplexers and generate the timing pulses.

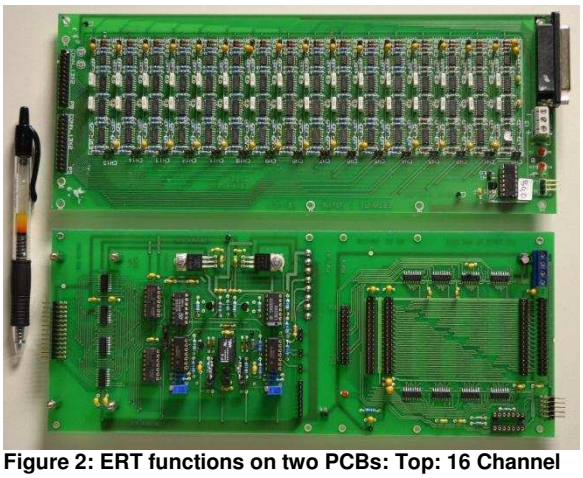

Figure 2: ERT functions on two PCBs: Top: 16 Channel amplifier with sample and hold. Bottom: Current source and multiplexers

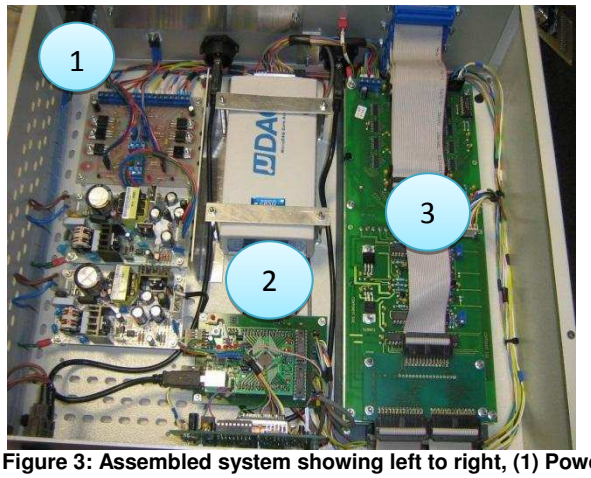

Figure 3: Assembled system showing left to right, (1) Power supplies, (2) DAQ and MCU and (3) ERT PCBs 1 and 2. (Wafer PC normally mounted above DAQ - not installed)

The Freescale MCU (GB60) controls the current pulse timing and electrode selection, which is specified by a sequence table downloaded from the PC. During frame capture, a bi-directional current pulse is injected into each of the drive electrode pairs specified in the sequence table. The resultant voltages between all the adjacent measuring pairs are sampled (simultaneously), amplified and then measured by the DAQ and transmitted to the PC via USB. Other measurement combinations (e.g. opposites) can be selected by installing an alternative "key-card". This sequence is repeated until frame capture is terminated. Refer to Randall (2010) for a more detailed description of this procedure.

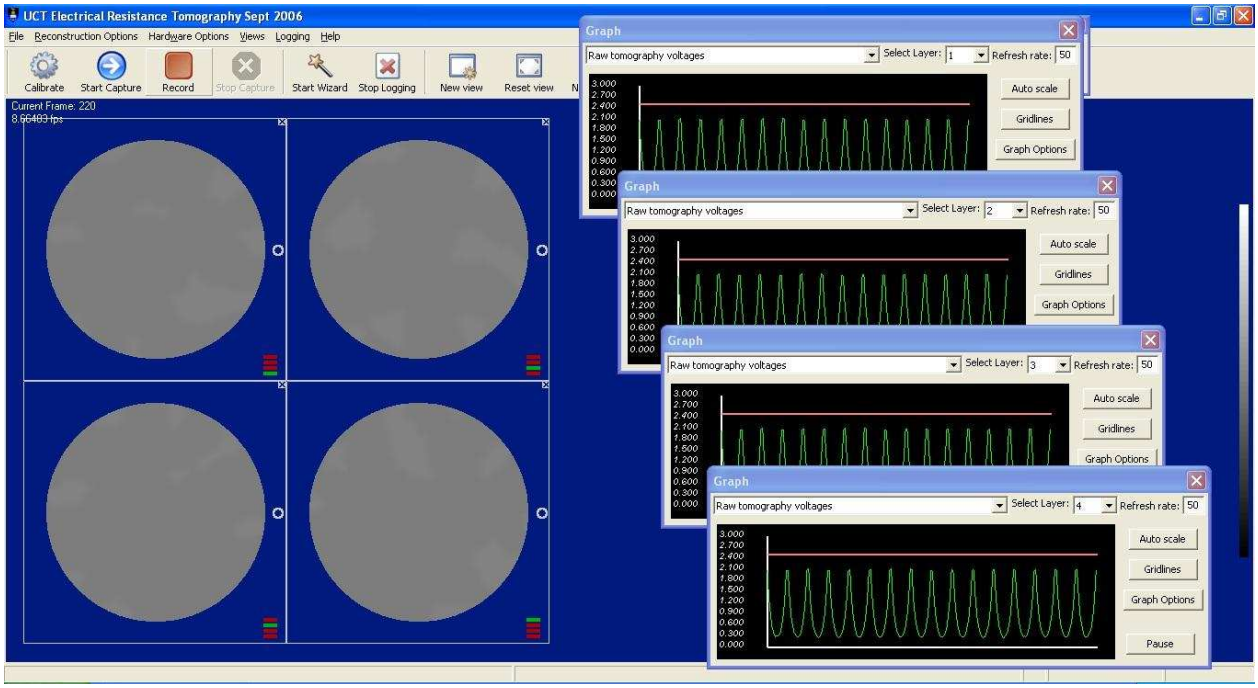

Figure 4: Typical screen output from the OLT code during frame capture. The 2D on-line reconstructions are from adjacent pairs data sets acquired from four independent rings of 16 electrodes. The uniform grey scale images (black to white representing a 10% change in conductivity) indicate a homogeneous medium in the measuring vessel (i.e. a saline solution of 100mg/l NaCl).

Much effort has gone into reducing noise in the recorded data. This is influenced by power supplies (and location), cabling (internal and to the electrodes), internal layout of components, current pulse and measurement timing as well as the design of the PCBs (particularly the amplifiers). The amplifier (PCB 1 in Figure 1) is now flood-filled with grounded copper on both layers and a grounded aluminium plate separates it from the current source and multiplexer board mounted above. This has resulted in the average standard deviation of the noise being reduced to less than 1mV when measured under laboratory test conditions. In practical operation, noise levels may be up to an order of magnitude higher and data frames need to be averaged to achieve acceptable results. Caution should be exercised when applying frame averaging. In situations where the system under investigation is not at steady state (e.g. a turbulent bubble column) the resultant reconstructed images may be degraded by averaging. Variable speed motor drives (inverters) used to drive pumps and mixers are particularly prone to generating noise and it is believed that the noise may be coupled to the electrodes via the liquid stream. Electrical suppression of the drives and motors can reduce this problem.

The plots in Figure 5 show the un-calibrated "U curve" data set typical of the adjacent pairs measurement sequence and the standard deviation of the noise for every data point calculated over 50 frames.

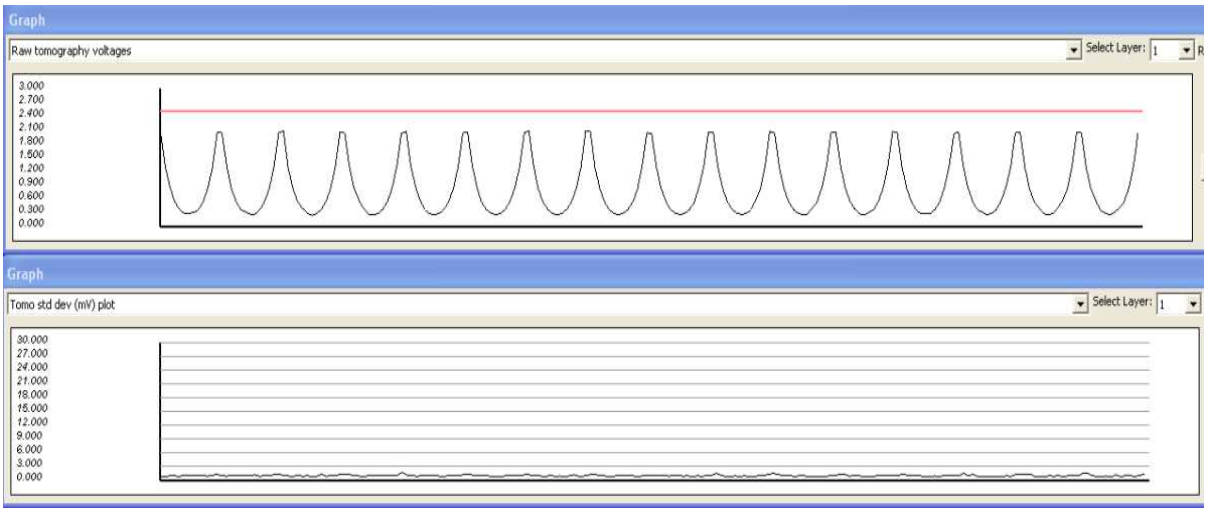

Figure 5: Top: Un-calibrated "U" curves from adjacent pairs measurement sequence (peaks at approx 2V). Bottom: Standard deviation (measured over 50 frames) of noise on frame data when driving a resistor network simulating a ring of 16 electrodes. (Standard deviation < 1mV)

3 MEASUREMENT CAPABILITIES

The reconstructed images presented below were generated by the "On-line Tomography" (OLT) software used to control the system described by Long (2006). The reconstruction algorithm was optimised for speed and real time visualization. Spatial representation is not accurate and resultant images should be regarded as first approximations. This size distortion is most pronounced when reconstructing data sets recorded in cases where step changes in conductivity are present, e.g. the insulating phantom considered below. More accurate representation of size may be obtained by off line processing. The data sets presented below do, however, give a realistic indication of the system capabilities.

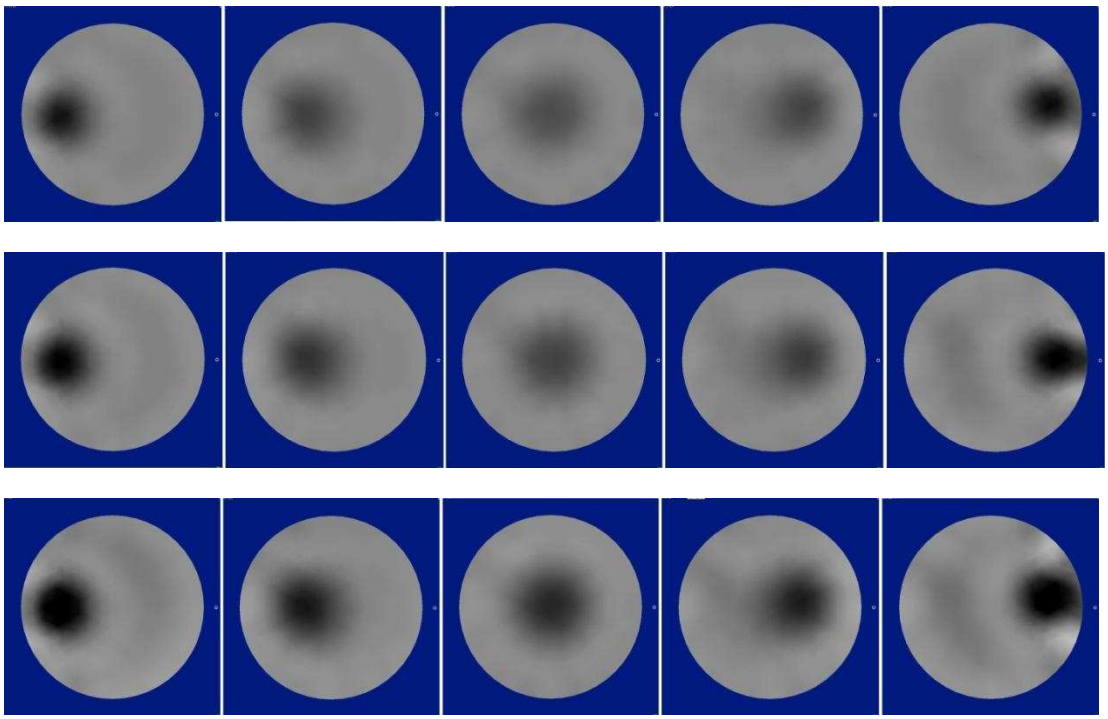

Figure 6: Adjacent pairs 2D reconstructions of a 25 mm insulating phantom in 290 mm diameter measuring tank. Scale represents conductivity change to go from black to white. (a - top) Grey scale 50%, (b - mid) Grey scale 40%, (c - bot) Grey scale 30%

Reconstructions of an insulating phantom (25mm rod) as it is moved across the diameter (D=290mm) of a measuring tank filled with a 100mg/l NaCl solution are presented in Figure 6. The grey scale range (%) specified indicates change in conductivity that results in a change from black to white on the reconstructed image. Each successive row represents a series displayed at scales of 50, 40 and 30%. As is typical of adjacent pairs measurements, sensitivity is reduced at the centre. The position is, however, accurately defined.

The spatial resolution for ERT systems is generally considered to be in the order of 5% of the measuring tank diameter. Figure 7 shows reconstructions of a 10 mm (3.5% of tank diameter) insulating rod in the 290mm diameter tank. It is clearly visible when the grey scale range is set to 6%, and at a higher contrast when the range is reduced to 4%. More noise becomes evident as the range is decreased.

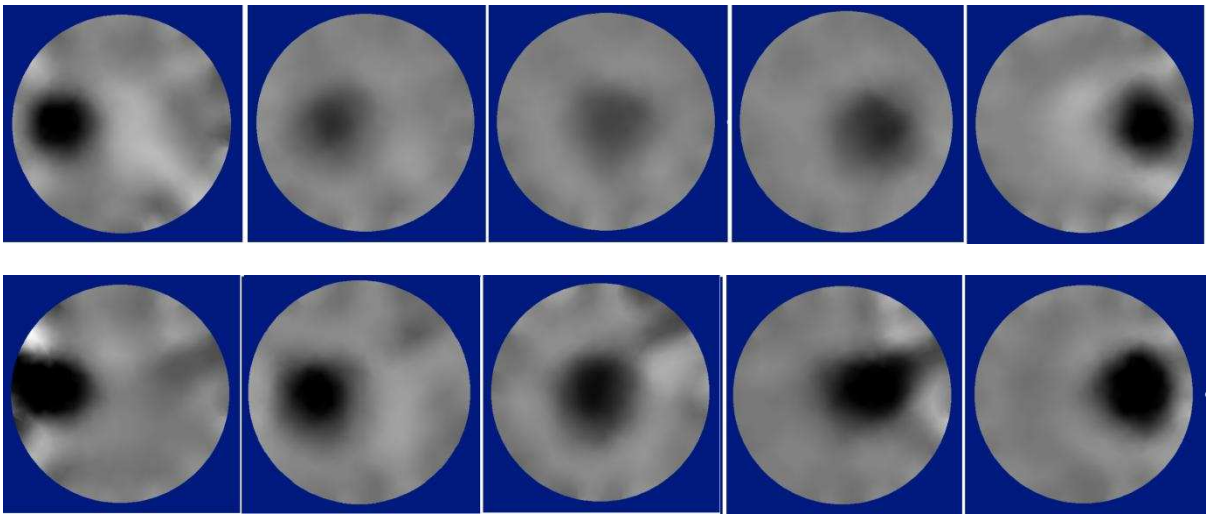

Figure 7: Adjacent pairs 2D reconstructions of a 10 mm insulating phantom in 290 mm diameter measuring tank, (a - top) Scale = 6%, (b - bot) Scale = 4%

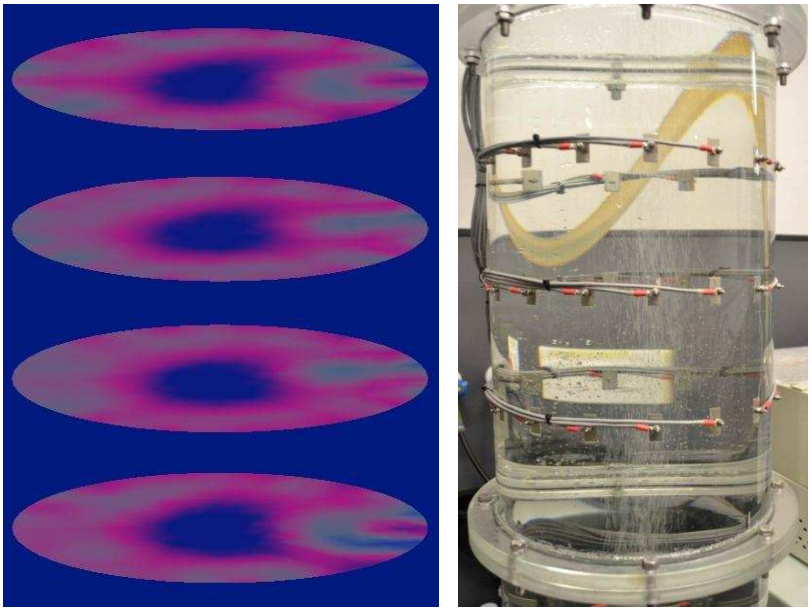

Figure 8: The images reconstructed from measurements of a very small bubble stream (air flow = 1 l/m) demonstrate operation at close to the instrument's maximum resolution.

The images obtained from a bubble column, shown in Figure 8, demonstrate the operation of the system at close to its maximum resolution. The bubble stream was generated by a very low air flow rate (1 l/m), where turbulence was minimal. To achieve the visualization, the conductivity scale range had to be reduced to 2%. It clearly shows that the measuring system is sufficiently sensitive to be able to resolve changes in conductivity in that range.

4 FLOTATION COLUMN APPLICATION

Flotation columns are used extensively in minerals processing for recovery of minerals from the tailings (i.e. waste). The extraction of the vast majority of the world's copper from the mined ore (i.e. more than $2x10^9$ tons/year) is one such application. In this process the hydrophobic copper in the finely milled ore attaches to small bubbles and is carried out at the top of the column in the froth. Bubbles are generated by aeration using various types of air spargers, and surfactant is added to reduce surface tension which inhibits coalescence and results in a typical bubble size range of 1 to 3mm diameter. In optimising the operation of such columns, both the distribution of the gas (bubbles) and the actual size distribution of the bubbles are important. From the size distribution and total gas hold-up, the surface area flux can be calculated and this has been shown to be directly related to the efficiency of mineral recovery in flotation cells by Gorain et al (1997). The overall gas hold-up is easily determined by measuring the liquid level change when the air supply is shut off. However, from this measurement alone, the distribution of the gas in the column is unknown. Many different methods have been used to estimate the distribution of the gas in columns and these have been extensively documented by Kourunen et al (2011). These include mechanical sampling systems and conductivity measurements, which are both invasive. Kourunen has demonstrated that ERT is a viable technique for these measurements and has the significant advantage of being non-invasive. Electrical tomography measurements do not have sufficient resolution to enable bubble size distribution to be determined. The size distribution can, however, be measured with an optical capillary probe, described by Randall (1989). Application of ERT, together with the bubble size measurements can provide valuable information for designing, modelling and optimising flotation systems.

The brief results presented below indicate that the low cost UCT current pulse ERT system can be used to determine air distribution in such columns.

4.1 Gas Distribution in Measurements

Various measurements were made on a laboratory flotation column (D = 290 mm, H = 1500 mm) with ERT measurement electrodes fitted as shown in Figure 9 below.

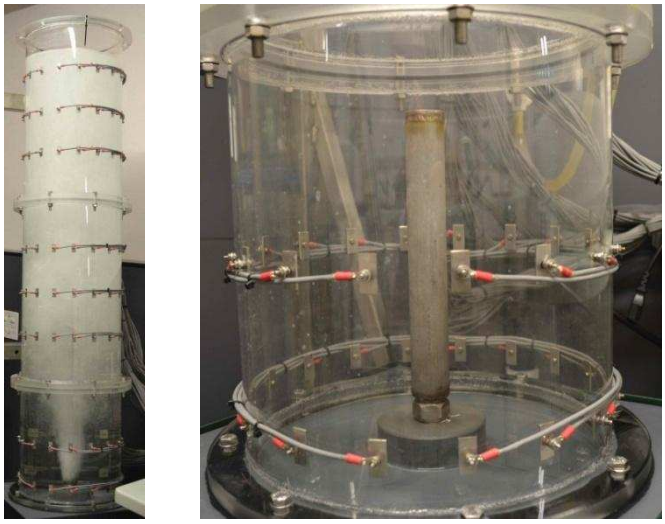

Figure 9: Bubble column (h=1500mm, D=290mm) and sintered metal air sparger used in tests. The column is fitted with 8 rings of 16 electrodes.

Figure 10 shows images, reconstructed in real time by the OLT software, of bubble plumes resulting from air flow rates of (a) 5 l/m and (b) 20 l/m, injected into the column using a sintered metal sparger as shown in Figure 9. The 2D reconstructions are from 4 rings of 16 electrodes. At the lower flow rate, the bubbles rise vertically with some dispersion, whereas turbulence results at higher flow rates. Visual observation and photography verify these results.

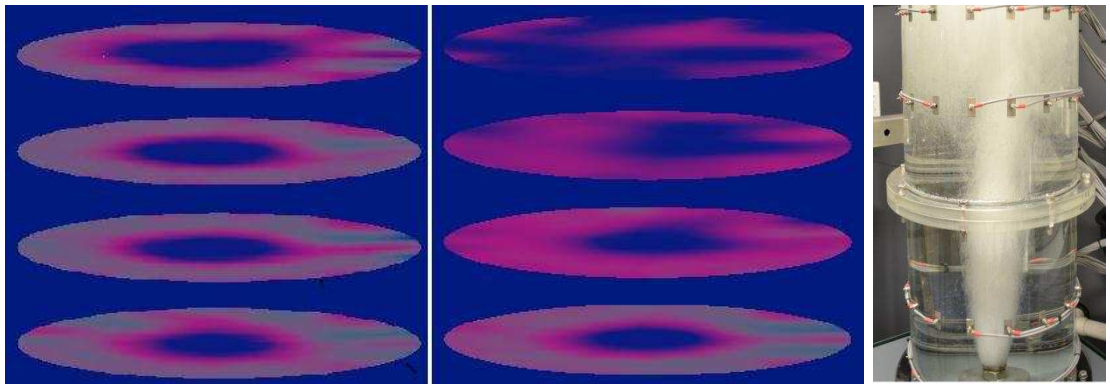

(a) (b) (c)

Figure 10: Reconstructed images of a bubble plumes from a sintered metal sparger showing dispersion due to turbulence at the higher flow rate. (Air vertical: (a) 5 l/m, and (b) 20 l/m; scale 6%)

Similar measurements were repeated with the column inclined at 5° from the vertical, which resulted in the bubble stream being biased toward the side of the column. This is clearly visible in the two sets of reconstructions shown in Figure 11 and was again verified photographically and by visual observation.

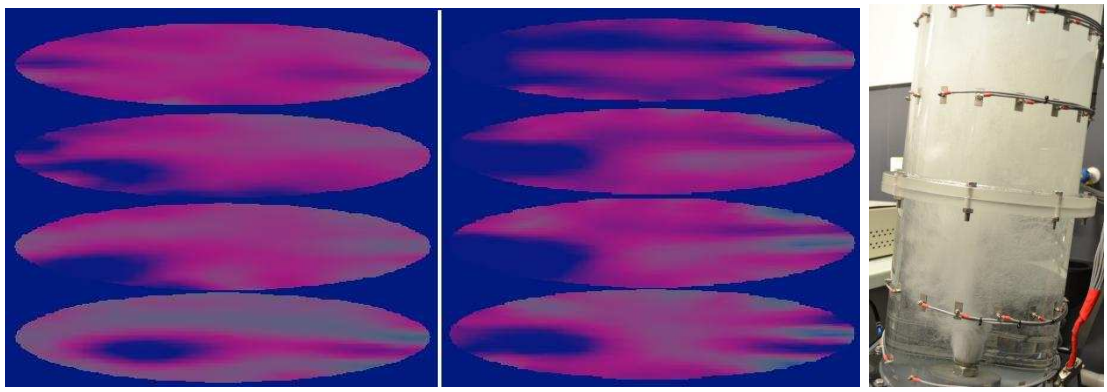

(a) (b) (c)

Figure 11: Reconstructed images of bubble steam in column inclined at 5 deg
Conductivity scale = 6% (a) Air flow = 5 l/m (b) Air flow = 10 l/m (c) Inclined column

The two reconstructions shown in Figure 12 compare the images generated by the OLT code to an off-line 3D reconstruction performed using the EIDORS code, Polydorides, 2002. The "image stack" was reconstructed from adjacent pairs measurements acquired independently from thee electrode rings, whereas the data for the EIDORS reconstruction was acquired using opposite pairs current injection and adjacent pairs measurements. The following measurement sequence was followed: inject on layer 1, measure on layers 1, 2 and 3, inject on layer 2, .measure on layers 1, 2 and 3, inject on layer 3, measure on layers 1, 2 and 3 (i.e. 9 x 256 measurements). The frame rate for the 3D data set is therefore 3 times slower than for the 3 sets of 2D data. The total reconstruction time for the three sets of 2D data is < 10mS on the Intel Atom processor, whereas the off-line 3D (EIDORS / MATLAB) reconstruction took

approximately 1 minute on a 3GHz AMD CPU. Although the results are similar, it is suspected that the 3D data sets could yield more information if a more appropriate image prior and a finer mesh is used in the reconstruction algorithm.

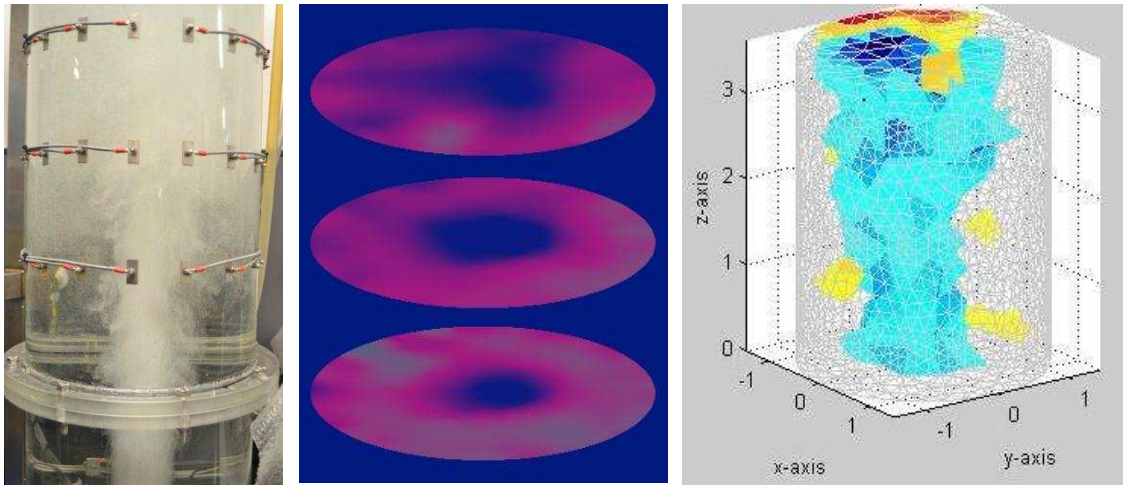

Figure 12: Comparison of high speed on-line 2D and off-line 3D reconstructions of air plume in bubble column (air flow = 10 l/m). Images reconstructed from measurements on 3 rings of 16 electrodes.

4.2 Bubble Size Determination

Bubble size distributions can be determined by a capillary optical system first described by Randall et al (1989). Bubbles are drawn through a capillary probe, which is inserted into the bubble column, and optically detected by two LED / Photo-transistor pairs as illustrated in Figure 13. If the rate is kept below 2 m/s, it can be assumed that the bubble forms a cylinder in the capillary.

The pulse width (measured by either detector) is proportional to the length of the air cylinder and the velocity is calculated from the time interval between the leading edges of the pulses from the bottom and top detectors. The volume is proportional to the "length" pulse and inversely proportional to the velocity pulse (high velocity results in expansion under vacuum). Typically, data from two to three thousand bubbles are recorded by a MCU/Timer system and transmitted to a PC for analysis. This data plus the total air volume, measured with a burette, yields a size distribution histogram as shown in Figure 13. The results obtained using this technique compare favourably with an image processing method developed by Gomez (2004).

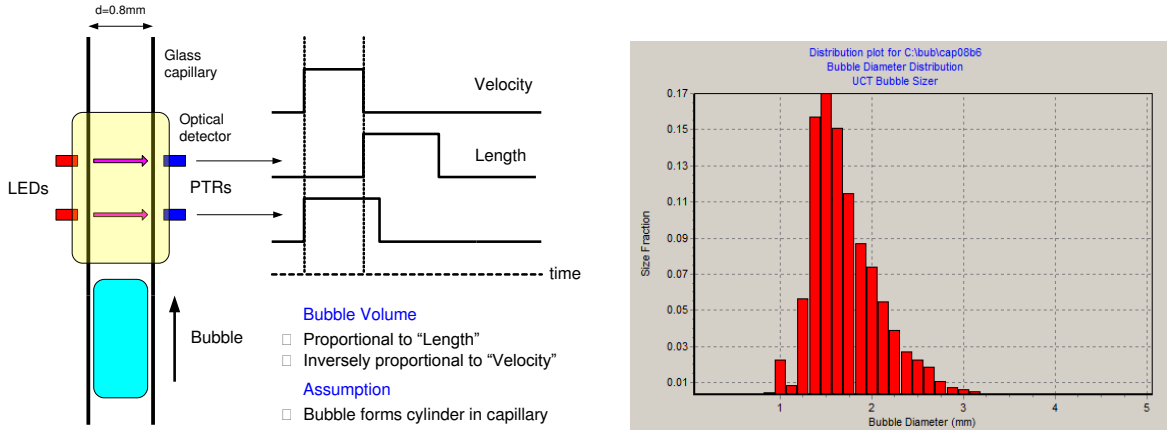

Figure 13: Optical capillary method for bubble size measurements

From this histogram, the Sauter mean diameter (d_{32}) of the bubbles (average bubble size which has the same area to volume ratio as bubbles present in the column) may be calculated using equation 1.

$$d_{32} = \frac{\sum n_i d_i^3}{\sum n_i d_i^2} \ [m] \tag{1}$$

Since the superficial velocity (i.e. volume flow rate / column surface area) is known from direct measurement, bubble surface area (S_b) flux may be calculated using equation 2:

$$S_b = \frac{6J_g}{d_{32}} \ [s^{-1}] \tag{2}$$

Solving equations 1 and 2 for the size distribution shown in Figure 13 yields a value of 1.9 s^{-1}. This parameter has been shown to be linearly related to the recovery of the mineral in a flotation column (or tank cell) by Gorain et al (1997) and has been used extensively in the design and simulation of these systems since that time.

5 CONCLUSIONS AND FUTURE DEVELOPMENT

The ERT system described in this paper is high speed, low cost and the primary functions easily implemented on only two circuit boards. This latest version of the system has improved signal to noise performance and exhibits low drift. The data presented verifies that the system can provide useful data-sets for evaluating the performance of bubble columns and complements the surface area measurements determined by the optical size distribution instrument. Improved reconstruction algorithms are likely to provide more quantitative information and yield useful engineering parameters for designing flotation cells.

The system electronics have been described in detail in several publications referenced in this paper. The re-design of the 3D multiplexing system, described by Wilkinson et al (2006), in a smaller footprint to complement the hardware described in this paper is currently being investigated. An open source version of the software is planned which will at least initially implement the frame capture and record functions. A clearly defined user interface will be provided for adding reconstruction routines.

4 ACKNOWLEDEMENT

The authors would like to thank Prof. J-P Franzidis for his explanations regarding minerals flotation processes.

6 REFERENCES

RANDALL, E.W., WILKINSON, A.J., CILLIERS, J.J., XIE, W., NEETHLING, S.J., (2001), Current pulse technique for electrical resistance tomography measurements, Proceedings of *2nd World* Congress on Industrial Process Tomography. Hanover, Germany, pp. 493-501.

WILKINSON, A.J., RANDALL, E.W., LONG, T.M., COLLINS, A., (2006), The design of an ERT system for 3D data acquisition and a quantitative evaluation of its performance, Meas. Sci. and Technol., 17, pp 2088-2096

RANDALL, E.W., WILKINSON, A.J., LONG, T.M., DUGGIN, K.E., HAUSLAB, K.H, (2010),

An improved design for a Current Pulse Electrical Resistance Tomography System, Proceedings of 6th World Congress on Industrial Process Tomography, Beijing, China..

LONG, T.M., (2006), An on-line velocity profiling system using Electrical Resistance Tomography, MSc thesis, University of Cape Town.

KOURUNEN, J., NIITTI, T., HEIKKINEN, L.M., (2011), Application of three-dimensional resistance tomography to characterize gas holdup distribution in laboratory flotation cell. Minerals Engineering 24, pp 1677-1686

RANDALL, E.W., GOODALL, C.M., FAIRLAMB, P.M., DOLD, P.L., O'CONNOR, C.T,(1989),
A method for measuring the size of bubbles in two and three phase systems,
Randall,E.W., Goodall, C.M., Fairlamb, P.M., Dold, P.L. and O'Connor, C.T.
Journal of Phys E Sci Instrum. 22, pp 827-833

STEPHENSON, D. R., YORK, T.A., MANN, R., (2007), Performance and Requirements of Process ERT Instruments. In Proc., 5th World Congress of Industrial Process Tomography, Bergen, Norway

GORAIN, B., FRANZDIS, J.P, MANLAPIG, E.V.,(1997), Studies on impeller type, impeller speed, and air flow rate in an industrial flotation cell. Part 4. Effect of bubble surface area flux on flotation performance. B.K. Gorain, Minerals Engineering, Vol 10, No 4, pp 367-379

POLYDORIDES, N.P., LIONHEART W.R.B., (2002) 'A MATLAB toolkit for three dimensional electrical impedance tomography: A contribution to the EIDORS project', Meas. Sci. Technol. 13, pp. 1871-1883

GOMEZ, C.O, HERNANDEZ-AGUILAR, J., FINCH, J.A. (2004), A comparison between capillary and imaging techniques for sizing bubbles in flotation systems, Minerals Engineering 17, 53-61